

Divergence in the face of gene flow in two *Charadrius* plovers along the 2 Chinese coast

4 Xuejing Wang^{1§}, Pinjia Que^{2§}, Gerald Heckel^{3,5}, Junhua Hu⁴, Xuecong Zhang¹,
Chung-Yu Chiang⁶, Qin Huang¹, Simin Liu¹, Jonathan Martinez⁷, Nan Zhang¹, Emilio
6 Pagani-Núñez¹, Caroline Dingle⁸, Leung Yu Yan⁸, Tamás Székely^{1,9}, Zhengwang
Zhang², Yang Liu^{1*}

8

1. State Key Laboratory of Biocontrol, Department of Ecology, School of Life
10 Sciences, Sun Yat-sen University, Guangzhou 510275, China
2. Ministry of Education Key Laboratory for Biodiversity and Ecological
12 Engineering, College of Life Sciences, Beijing Normal University, Beijing,
100875, China
3. Institute of Ecology and Evolution, University of Bern, Baltzerstrasse 6, 3012
14 Bern, Switzerland
4. Chengdu Institute of Biology, Chinese Academy of Sciences, Chengdu 610041,
16 China
5. Swiss Institute of Bioinformatics, Genopode, 1015 Lausanne, Switzerland
6. Department of Environmental Science, Tunhai University, Taichun, Taiwan,
20 China
7. 14, bis rue des Temples 45240 La Ferté Saint Aubin, France
8. School of Biological Sciences, The University of Hong Kong, Hong Kong
22 S.A.R., China
9. Milner Center for Evolution, Department of Biology and Biochemistry,
24 University of Bath, Bath BA1 7AY, UK

26 **Running title:** Incipient speciation in *Charadrius* plovers

Total words (without reference): 7930

28 **References** □ 133

30 *Correspondence: Yang Liu, School of Life Sciences, Sun Yat-sen University,
Guangzhou, China. Email: liuy353@mail.sysu.edu.cn;
32 § These authors contributed equally to this work.

34

Abstract

36 Speciation with gene flow is an alternative to the nascence of new taxa in strict
allopatric separation. Indeed, many taxa have parapatric distributions at present. It is
38 often unclear if these are secondary contacts, e.g. caused by past glaciation cycles or
the manifestation of speciation with gene flow, which hampers our understanding of
40 how different forces drive diversification. Here we studied genetic, phenotypic and
ecological aspects of divergence in a pair of incipient species, the Kentish (*Charadrius*
42 *alexandrinus*) and the white-faced Plovers (*C. dealbatus*), shorebirds with parapatric
breeding ranges along the Chinese coast. We assessed divergence based on
44 molecular markers with different modes of inheritance and quantified phenotypic and
ecological divergence in aspects of morphometric, dietary and climatic niches. These
46 analyses revealed small to moderate levels of genetic and phenotypic distinctiveness
with symmetric gene flow across the contact area at the Chinese coast. The two
48 species diverged approximately half a million years ago in dynamical isolation and
secondary contact due to cycling sea level changes between the Eastern and
50 Southern China Sea in the mid-late Pleistocene. We found evidence of character
displacement and ecological niche differentiation between the two species, invoking
52 the role of selection in facilitating divergence despite gene flow. These findings imply
that the ecology can indeed counter gene flow through divergent selection and thus
54 contribute to incipient speciation in these plovers. Furthermore, our study highlights
the importance of using integrative datasets to reveal the evolutionary history and
56 underlying mechanisms of speciation.

KEY WORDS: allopatric speciation, character displacement, gene flow, hybridization,

58 stable isotope analysis, ecological niche

1 INTRODUCTION

60 Understanding how strongly the evolutionary processes, i.e. selection, gene flow and
genetic drift shape the divergence of closely related species has been a long-standing
62 interest in evolutionary biology (Coyne & Orr 2004; Feder et al. 2013; Nosil & Feder
2012; Wagner et al. 2012; Wolf & Ellegren 2017). Allopatric speciation is
64 conventionally considered as the prevalent mode of speciation in which physical
barriers completely restrict gene flow between two populations, facilitating the initiation
66 of divergence through genetic drift or selection (Bernardi et al. 2008; Carson & Clague
1995; Mayr 1963). If populations remain isolated for a period long enough after
68 divergence has been established, then this divergence could be maintained even in
the presence of gene flow after secondary contact (Le Moan et al. 2016; Zhou et al.
70 2016).

72 An increasing number of studies have shown that divergence can arise and be
maintained due to selection imposed by heterogeneous environments despite the
74 constraining effect of gene flow (Martin et al. 2013; Morales et al. 2017). Under this
scenario, divergent selection or ecologically-mediated sexual selection operating on
76 certain (“magic”) traits can lead to reproductive isolation, and incompatibilities in a few
“speciation genes” may be enough to constrain the homogenizing effect caused by
78 gene flow even at an early stage of speciation (Fitzpatrick et al. 2015; Nosil & Schlüter
2011; Slatkin 1973). For instance, different host plant preferences result in different
80 digestive and physiological traits in *Timema* walking-stick insects (Nosil 2007).
Locally-adapted phenotypes in body size are related to swimming and foraging
82 ecology in guppies (*Poecilia reticulata*), which can maintain population diversification
in the face of extensive gene flow (Fitzpatrick et al. 2015). Though evidence of
84 speciation with gene flow is accumulating (Martin et al. 2013; Morales et al. 2017;
Schlüter 2009; Seehausen et al. 2014), to what extent a balance between selection
86 and gene flow can drive divergence remains largely unknown. This might be
interesting in populations with high propensity of range-wide gene flow such as in

88 waterfowl (e.g. Liu et al. 2012) and shorebirds (Eberhart□Phillips et al. 2015; Küpper et al. 2012).

90

Shorebirds are a group of migratory species with remarkable movement ability.

92 Seasonal migration may increase the probability of individual dispersal between populations (Arguedas & Parker 2000; Procházka et al. 2011) and consequently drive

94 frequent gene flow between geographically distant populations (Peters et al. 2012;

Winker et al. 2013). Direct evidence using tracking approaches confirmed that

96 extremely long-distance gene flow can be mediated through individual movements among remote breeding colonies of pectoral sandpipers (*Calidris melanotos*)

98 (Kempenaers & Valcu 2017). Range-wide phylogeographic studies also revealed extensive gene flow in several migratory shorebird species (e.g. Trimbos et al. 2011;

100 Küpper et al. 2012; Miller et al. 2014). This may result in weak genetic structure across a species and consequently prevent population-level divergence (Eberhart□Phillips et

102 al. 2015; Jackson et al. 2017).

104 In this study, we test the role of ecology and gene flow on the divergence of two shorebird species, the Kentish Plover (*Charadrius alexandrinus*) and the white-faced Plover (*C. dealbatus*) (Figure 1) . *C. alexandrinus* breeds in coastal areas and inland lakes in Europe, Asia and North Africa (del Hoyo et al. 2016). A previous study

106 uncovered low genetic differentiation of *C. alexandrinus* across the Eurasian continent, and also between continental and island populations in East Asia (Küpper et al. 2012).

108 110 *C. dealbatus* was formerly regarded as a subspecies of Kentish plover (Hartert & Jackson 1915; Swinhoe 1870). Breeding sites of *C. dealbatus* were documented along the coast of China from Fujian to Hainan Island, and in south middle Vietnam (BirdLife International 2016), yet its geographic range is uncertain (Kennerley et al. 2008).

112 114 Previous studies have found subtle but diagnosable differences in morphometric, plumage and behavioral traits between the two taxa (Figure 1d), leading to the erection of *C. dealbatus* as a full species (Bakewell & Kennerley 2008; Kennerley et al. 2008; Rheindt et al. 2011). The first genetic investigation on the relationship between these

118 two taxa provided no evidence of genetic differentiation and concluded that these
species may only differ in a few genomic regions (Rheindt et al. 2011). Although based
120 on a handful of genetic loci, this finding is noteworthy as it raises a probability of
divergence in the face of gene flow between these two young species.

122

Here we provide comprehensive data from multiple sources to explore divergence
124 patterns between these two species of plovers. We carried out extensive sampling on
breeding populations covering the potential area of contact along the Chinese coast.
126 We obtained genetic polymorphism data from multiple markers with various mutation
rates, i.e. mitochondrial DNA, exons and autosomal microsatellites. Using these new
128 datasets, it is possible to estimate the intensity and direction of gene flow (Hey &
Nielsen 2004; Won & Hey 2005) as well as other important demographic parameters
130 such as the effective population size (N_e) and the timing of divergence (reviewed in
Hey 2006) between *C. alexandrinus* and *C. dealbatus*. Because it is difficult to directly
132 quantify divergent selection, inference from the comparisons of traits which are
potentially targets of selection are necessary to offer hints on selective mechanisms in
134 maintaining divergence (Hoskin & Higgle 2010; Lande 1982; Nosil 2007). By collecting
data on morphology, diet, and environmental niche, we attempt to 1) characterize
136 geographic variation in genetic and phenotypic traits in the two plovers, 2) estimate
demographic history and intensity of gene flow, and 3) infer the role of multiple factors,
138 i.e. geographical premating isolation and gene flow during divergence between these
two taxa. Taken together, our investigation provides new insights into the evolutionary
140 history of two incipient bird species.

142 **2 MATERIALS AND METHODS**

DNA sample collection

144 We mainly collected samples along the eastern coastal area of China (Fig 1a), and
also obtained samples from the two biggest continental islands, Taiwan and Hainan,
146 as well as two small islands that are close to the Chinese coastal line (Zhoushan and

Jinmen). Sampling sites were separated by approximately 200-250 km along a 2,300
148 km transect, spanning almost the entire Chinese coastline. Further, one high altitude
150 population (breeding at 3 350 m a.s.l.) near Qinghai Lake was sampled as an inland
outgroup. Breeding individuals were captured using a funnel-trap method described in
152 Székely et al. (2008) between March and July in 2014-2015. For each nest, blood
samples of the breeding pair or a chick were collected. Tissue samples were also
154 obtained from dead individuals found in the field. Species identification during
sampling was based on the summary of plumage characters, morphometric, and
156 ecological differences between *C. alexandrinus* and *C. dealbatus*, as described in
Kennerley et al. (2008). Overall, we collected samples from 454 individuals from 19
breeding sites. All bird-capture and sampling were performed with permission from the
158 respective authorities (Mainland China: Beijing Normal University to PJQ and Sun
Yat-sen University to YL; Taiwan: Changhua County Government, New Taipei City
160 Government and Kinmen County Government to ZYJ).

162 **Morphometric analysis**

For each adult individual, four basic morphometric measurements were taken: body
164 mass, wing length, tarsus length and bill length. Body mass was measured with an
electronic scale (± 0.01 g). Wing length (flattened) was measured with a wing ruler (± 1
166 mm). Bill length to skull and tarsus lengths were measured using vernier callipers (\pm
0.01 mm). Measurements were taken by QH, PJQ and ZYJ following the standard
168 described in Redfern & Clark (2001). To avoid potential biases, some individuals were
measured twice or three times among these authors to make sure there was no
170 significant difference ($p < 0.05$, between 20 – 30 trials) among them at the beginning
and end of the fieldwork in the year 2014-2015.

172

We carried out principle component analysis (PCA) for the four traits to visualize the
174 variation of morphometric data. Analyses of covariance (ANCOVAs) were conducted
based on the PCA results to test statistical significance. We carried out t-tests between
176 species for each measurement. Pairwise morphological difference Q_{ST} based on PC1

178 scores from PCA were calculated following Storz (2002) and plotted against linear
distances between coastal populations. All aforementioned analyses were performed
in PAST 3.12 (Hammer *et al.* 2001).

180

DNA Sequencing and microsatellite genotyping

182 We extracted genomic DNA using Tiangen Blood & Tissue Genome DNA Kits,
following manufacturer protocols (Tiangen, Beijing, China). DNA quality was measured
184 with NanoDrop 2000 (Thermo Scientific, USA). Three mtDNA loci, partial ATPase
subunit 6/8, partial D-Loop of the mitochondrial control region (CR) and NADH
186 dehydrogenase subunit 3 fragment (ND3), were amplified for all samples using primers
from Rheindt *et al.* (2011). PCR reactions for mtDNA amplification were carried out in
188 20 μ l volumes containing 1X PCR buffer (Takara Shuzo, Japan), 10-50ng DNA
template, 0.5 unit Taq DNA Polymerase (Takara Shuzo, Japan), 1.0 μ M of each primer,
190 2.0 mM of each dNTP and 1.0 μ M MgCl₂. We also sequenced 14 autosomal and two
Z-linked exonic loci (designed from Liu *et al.* 2018) for a subset of 40 individuals
192 representing both species and several populations within species. PCR for nuclear loci
had higher concentration of dNTP at 4.0 mM and 2.5 μ M for MgCl₂ and PCR cycling
194 profiles are listed in Table S3. Each PCR product was checked on a 1% agarose gel
and then sequenced on ABI3730XL (Applied Biosystems, USA) served by MajorBio,
196 Shanghai, China.

198 We genotyped all individuals at 22 autosomal microsatellite markers (mst) mostly from
Küpper *et al.* (2007) but with C204 from Funk *et al.* (2007) and Hru2 from Primmer *et al.*
200 (1995). Microsatellite loci were amplified using three multiplex PCRs with respective
cycling profiles (Table S3). Each PCR was in a total volume of 15 μ l containing 1X
202 HotStart buffer (Tiangen), 10ng DNA template, 1 unit Multi HotStart DNA Polymerase
(Tiangen), 0.4 μ M of each fluorescently labeled primer, 2.0 mM of each dNTP and 2.0
204 μ M MgCl₂. Multiplex PCR products and associated genotypes were isolated on
ABI3730XL (Applied Biosystems, USA) served by Invitrogen, Shanghai, China and

206 their length was determined using GeneMapper software v.3.7 (Applied Biosystems)
207 against an internal size standard (GeneScan-500LIZ; Applied Biosystems).

208

Genetic diversity and population structure analyses

210 For DNA sequence data, we aligned each mitochondrial or nuclear locus using the
211 CLUSTAL W algorithm implemented in MEGA v.6.06 (Tamura et al. 2013), and the
212 alignment was checked by eye and manually edited if needed. For nuclear DNA
213 sequence data, we first used PHASE 2.1.1 (Stephens et al. 2001) to reconstruct
214 haplotypes of nuclear sequences with heterozygous sites. Each run was set to 10,000
215 iterations, 100 burn-in and 10 thinning intervals. For both mtDNA and nuclear loci,
216 basic genetic polymorphism statistics such as haplotype number h , haplotype diversity
217 H_d , number of segregating sites S , nucleotide diversity π and Tajima's D (Tajima 1989)
218 of each locus and each population were calculated in DnaSP 5.10.1 (Librado & Rozas
219 2009). Haplotype networks of each locus were constructed using a median-joining
220 algorithm (Bandelt et al. 1999) in PopART 1.7.2 (Leigh & Bryant 2015).

222 We used FreeNA (Chapuis & Estoup 2007) to check for the frequency of null alleles at
223 each microsatellite locus. Further tests for Hardy-Weinberg equilibrium and pairwise
224 linkage disequilibrium (LD) were carried out with Arlequin 3.1.1 (Excoffier et al. 2005).
225 Hardy-Weinberg equilibrium tests were run with 10,000 permutations. LD tests were
226 run for 100,000 steps of Markov chain. To obtain genetic diversity estimates, we
227 calculated observed heterozygosity (H_o) and expected heterozygosity (H_E) in GenAIEx
228 6.5.1 (Peakall & Smouse 2012).

230 We estimated population structure between species and among sampling sites within
231 species using several approaches. First, for mtDNA and microsatellites, we performed
232 analyses of molecular variance implemented (AMOVAs) in Arlequin to assess the
233 proportion of genetic variance explained by the different partition settings, e.g. (1) the
234 two species, (2) *C. alexandrinus* continental populations and Taiwan island
235 populations, *C. dealbatus*, (3) coastal populations (including Hainan Island), Qinghai

236 and Taiwan. Second, we also calculated pairwise Φ_{ST} and F_{ST} between breeding sites
237 for mtDNA and mst, respectively, and we derived significance levels using 10,000
238 permutations in Arlequin.

240 For microsatellite genotypes only, we carried out assignment analyses with two
241 model-based Bayesian approaches. First, we performed a Bayesian clustering
242 analysis using the admixture model with correlated allele frequencies implemented in
STRUCTURE 2.3.4 (Hubisz et al. 2009; Pritchard et al. 2000). Ten independent
244 analyses were run from $K=1$ to $K=8$ for 500,000 Markov chain Monte Carlo (MCMC)
245 generations with 100,000 burn-in. Replicate runs were combined using STRUCTURE
246 Harvester 0.6.94 (Earl 2012) and CLUMPP 1.1.2 (Jakobsson & Rosenberg 2007). The
most likely number of genetic clusters was also determined using Structure Harvester
248 using the criteria described in Evanno et al. (2005). Second, we used a Bayesian
clustering algorithm that takes the geographical coordinates of each sampling site into
250 account using the R package GENELAND 4.0 (Guillot et al. 2005). 1,000,000 MCMC
iterations were run with thinning set to 100 from 1 to 10 populations, with maximum
252 rate of Poisson process set to 100, uncertainty of spatial coordinates set to 0,
maximum number of nuclei in the Poisson–Voronoi tessellation to 300, and
254 independent Dirichlet distribution model for allele frequencies. With the same package,
the most likely number of clusters was determined based on their posterior density. To
256 confirm the consistency of the results, we repeated the MCMC simulation 10 times.

258 Furthermore, to determine the probability that an individual was a hybrid or a migrant,
259 we estimated the posterior probability of each individual based on multilocus
260 genotypes. First we used HYBRIDLAD 1.0 (Nielsen et al. 2006) to simulate 100
261 individuals of each species, F1, F2 and back-crosses in each direction from
262 microsatellite genotypes of 260 individuals with q-value higher than 95% in
STRUCTURE analysis. 100 simulated parents from each species and 100 F1 were
264 used to calculate the threshold for individual hybrid assignment in STRUCTURE
following Vähä and Primmer (2006). Finally, NewHybrid 1.1 (Anderson & Thompson

266 2002) was used to identify potential hybrid individuals. 100,000 burn-in followed by
267 400,000 sweeps were performed for both simulated and real data.

268

Demographic analysis

270 To infer the demographic histories of the two plover species, we applied Isolation with
271 Migration model (IM) (Hey & Nielsen 2007) analyses using the combined sequence
272 data set of 16 nuclear and three mtDNA loci based on 20 individuals of each species.
273 IM analysis allows the inference of genealogies under different demographic scenarios
274 and estimation of population genetic parameters, such as divergence times, effective
275 population sizes and migration rates between species since their divergence from the
276 common ancestor. The homologues Killdeer *Charadrius vociferus* sequences from
277 GenBank were used as outgroup. The substitution rate of each locus was calculated
278 using the method in Li et al. (2010). The ratio of net genetic distance of each locus
279 across ingroup–outgroup was calculated, compared with net distance of mitochondrial
280 cytochrome b (*cytb*) and then multiplied by the substitution rate for *cytb* (0.0105 ±
281 0.0005 substitution/site/mya, Weir & Schluter 2008). We used the Phi test (Bruen et al.
282 2006) for recombination within nuclear loci and no recombination was detected. We
283 implemented models in IMa2p (Sethuraman & Hey 2016), the parallel version of IMa2
284 (Hey 2010). For each analysis, we ran 48 MCMC chains for 2,500,000 steps of burn-in
285 followed by 500,000 genealogies saved, each recorded after 100 steps. Because IM
286 analysis only provides estimates of average gene flow since the divergence of the two
287 species, we used a Bayesian analysis in BayesAss 3.0.4 (Stephens & Donnelly 2003)
288 based on microsatellite genotypes to characterize the level of gene flow within recent
289 generations. We performed 10,000,000 iterations and 1,000,000 burn-in.

290

Ecological niche modeling and niche overlaps

292 To infer potential past range shifts induced by climatic changes, we carried out
293 ecological niche modeling (ENM) using Maxent 3.3.3k (Phillips et al. 2009). The
294 occurrence records of the two species of plovers were obtained from online databases
295 of the Global Biodiversity Information Facility (GBIF, <http://www.gbif.org/>), China Bird

296 Report (<http://www.birdreport.cn>) and our records during the sampling expeditions.
Further, eight bioclimatic variables (i.e., the mean diurnal range, isothermality,
298 minimum temperature of the coldest month, mean temperature of the warmest quarter,
annual precipitation, precipitation of the driest month and precipitation seasonality)
300 were obtained from the WorldClim database v.1.4 (Hijmans et al. 2005).

302 To explore niche similarity between the two species, we performed an ordination null
test of PCA-env in environmental (E)-space (Broennimann et al. 2012; Hu et al. 2016).
304 The PCA-env calculates the occurrence density and environmental factor density
along environmental (principal component) axes for each cell using a kernel smoothing
306 method and then uses the density of both occurrences and environmental variables to
measure niche overlap along these axes (Broennimann et al. 2012). An unbiased
308 estimate of Schoener's D metric was calculated for our data using smoothed densities
from a kernel density function to measure niche overlap between the two species that
310 is ensured to be independent of the resolution of the grid. Statistical confidence in
niche overlap values was then tested through a one-sided niche-similarity test
312 (Broennimann et al. 2012). All statistical analyses were performed in R 3.0.2 (R
Development Core Team 2013) using scripts available in Broennimann et al. (2012).
314 Details of ENM construction and niche-similarity tests are available in Appendix S1.

316 **Dietary niche differentiation inferred by stable-isotope analysis**

Because stable isotopic compositions of consumer tissues can be used to estimate the
318 relative contribution of assimilated dietary sources (DeNiro & Epstein 1978),
stable-carbon(C) and nitrogen(N) isotope analysis is widely used as a tool to study
320 avian dietary patterns (Hobson & Clark 1992; Pagani-Núñez et al. 2017). Carbon
isotope ratios differ between C3, C4 and CAM plants due to differences in the
322 photosynthetic pathways, and these differences are incorporated into an animal when
the plants are consumed and so can be used to infer information about dietary niches
324 (Hobson & Clark 1992). N isotopes are useful for identifying species/individuals which
occupy different trophic positions (high $\delta^{15}\text{N}$ implies higher trophic level; Chen et al.
326 2017). In order to compare dietary differences based on differences in $\delta^{15}\text{N}$ and $\delta^{13}\text{C}$
between the two species, we collected the outer pair of rectrices from seven adults per
328 site at eight sites: Qinghai Lake, Tangshan, Lianyungang and Rudong for C.

330 *alexandrinus*; Fuzhou, Shanwei, Zhanjiang, Dongfang for *C. dealbatus*. Since both
331 species perform a complete post-breeding molt within their breeding grounds (Ginn &
332 Melville 1983, personal observation), isotope ratios represent trophic level and habitat
333 preferences during the breeding period. We estimated niche width and overlap per
334 species using an isotopic Bayesian approach based on $\delta^{13}\text{C}$ and $\delta^{15}\text{N}$ profile. Detailed
information on lab procedures and statistical analyses can be found in Appendix S2.

336 **3 RESULTS**

Morphological differentiation

338 The two plover species showed subtle but significant differences for most
339 morphological traits (ANCOVA; $p < 0.001$, Figure 1) even though there was
340 considerable overlap in morphology between the species at the level of the individual
341 (Figure 1f). On average, *C. dealbatus* had a longer bill (17.91 ± 0.94 mm vs. $16.69 \pm$
342 1.06 mm in *C. alexandrinus*, $p < 0.001$, Figure 1b), longer wings (118.58 ± 2.90 mm vs.
343 115.59 ± 3.02 mm in *C. alexandrinus*, $p < 0.001$, Figure 1c), and larger body mass
344 (48.99 ± 3.26 g vs. 47.56 ± 3.73 g in *C. alexandrinus*, $p = 0.001$, Figure 1d, Table S5)
345 than those of *C. alexandrinus*. There was no difference in tarsus length between the
346 two species ($p = 0.962$). Individuals of *C. alexandrinus* from Taiwan Island were
347 heavier than continental populations of *C. alexandrinus* and *C. dealbatus* (both $p <$
348 0.001). Q_{ST} between coastal populations of *C. alexandrinus* and *C. dealbatus* was
349 negatively correlated with geographic distance ($R^2 = 0.293$, $p < 0.001$, Figure 1g).
350

Genetic diversity and population structure

352 We sequenced 357 individuals at all three mtDNA loci (224 *C. alexandrinus* and 133 *C.*
353 *dealbatus*, GenBank Accession No. xxxx-xxxx). For each site, sample size ranged
354 from 11 to 30 individuals. For each individual, we obtained in total 1729 base pairs (bp)
355 of mtDNA sequence, including 846 bp ATPase6/8, 505 bp D-loop and 378 bp ND3. *C.*
356 *alexandrinus* showed higher intraspecific genetic diversity than *C. dealbatus* (Table 1).
357 Haplotype networks show that in all loci, most individuals were sorted into two major

358 haplogroups, corresponding to the two species of plovers. One non-synonymous
359 substitution separated the two haplogroups at both ATPase6/8 and ND3 loci (Figure
360 2a). Moreover, a subset of samples containing 20 individuals of each species were
361 sequenced at 16 loci (range 440-902 bp for each locus; Table 1 and Table S1,
362 GenBank Accession No. xxxx-xxxx) for a total of 11,209 bp nuclear DNA sequence.
363 The haplotype networks from autosomal and Z-linked loci did not show strong patterns
364 of lineage sorting like mtDNA. The most common haplotypes were shared by both
365 species of plover (Figure 2b and S1). Moreover, both species showed the signal of
366 recent demographic expansion as detected by significant Tajima's *D* values (Table 1).

368 Overall genetic differentiation was significant and high in mtDNA data ($\Phi_{ST} = 0.506$, $p < 0.001$) and low at microsatellite loci ($F_{ST} = 0.036$, $p < 0.001$). For nuclear sequence
369 data, genetic differentiation between species was also significant at autosomal loci
370 ($\Phi_{ST} = 0.100$, $p < 0.001$) and particularly high at the Z-linked loci Z4 ($\Phi_{ST} = 0.726$, $p <$
371 0.001) and Z6 ($\Phi_{ST} = 0.309$, $p < 0.001$, Table S3). In the AMOVA analysis, we observed
372 the largest difference between groups when the data were partitioned by species (i.e.
373 *C. alexandrinus* and *C. dealbatus*), with this grouping explaining 49.7% of the variance
374 in mtDNA and 2.4% in the microsatellites ($p < 0.001$; Table 2). These were significantly
375 higher than the values of genetic variation when we partitioned samples as coastal vs.
376 island populations or coastal population vs. Qinghai vs. Taiwan populations. Within *C.*
377 *alexandrinus*, minor genetic differentiation was found between the inland population
378 (Qinghai Lake) and coastal populations (mtDNA $\Phi_{SC} = 0.042$, $p = 0.022$; mst $F_{SC} =$
379 0.021, $p < 0.001$). *C. alexandrinus* populations on Taiwan Island also shared
380 haplotypes with other coastal populations (mtDNA $\Phi_{SC} = 0.021$, $p = 0.146$); but were
381 significantly differentiated in microsatellites (microsatellite $F_{SC} = 0.016$, $p < 0.001$).
382

384 For microsatellite loci, 18 out of 22 markers were successfully genotyped. However,
385 four markers (Calex-04, 08, 19, C204) showed a large proportion of missing data, while
386 another four loci (Calex-11, 24, 26, 43) showed an estimated frequency of null alleles
387 over 10% and moreover one locus (Calex-35) showed H-W disequilibrium (Table S2).

388 Consequently, the aforementioned nine loci were removed from the dataset, making
389 genotypes at 13 loci of 402 (271 *C. alexandrinus* and 131 *C. dealbatus*) individuals for
390 the final microsatellite dataset for further analysis.

392 The results of the STRUCTURE analysis clearly showed two genetic clusters
393 representing each species (Figure 2d) and no obvious gradual transition along the
394 coastline that could be expected from a hybrid zone. The average *Delta K* value when
395 $K = 2$ was much higher than other options (Figure S2). Using georeferenced data in
396 GENELAND, our results corroborated the genetic clustering patterns inferred from
397 STRUCTURE. The posterior probability was 0.70 when $K = 2$ in contrast with the
398 posterior probability of 0.25 when $K = 3$. We visualized the GENELAND results in a
399 map with the probability distribution of posterior mode of class membership, which
400 further supports the separation between *C. alexandrinus* and *C. dealbatus* along the
401 China coast (Figure 2c). The divide between these two species was located between
402 Wenzhou and Fuzhou according to the GENELAND results, but it is unclear if these
403 two species come into contact or forms a putative hybrid zone in this region. Again, the
404 individuals from the sites in Taiwan were assigned to the cluster of *C. alexandrinus*
405 (Figure 2c).

406

Demographic history in two plovers

408 Isolation with migration analyses suggested that *C. alexandrinus* and *C. dealbatus*
409 diverged 0.56 (0.41 – 5.19) million years ago. Estimated migration rates in both
410 directions were significant ($p < 0.001$) with slightly higher gene flow from *C.*
411 *alexandrinus* into *C. dealbatus* (2.69 migrants per generation) than the vice versa (ca.
412 two migrants per generation). The estimated effective population size of *C.*
413 *alexandrinus* ($N_e \approx 1.59 - 4.44$ million) was about 8-10 times higher than for *C.*
414 *dealbatus* ($N_e \approx 0.15 - 0.52$ million).

416 The estimation of recent gene flow between the two species with BayesAss using
417 microsatellites also suggested bidirectional gene flow. Gene flow from *C. dealbatus* to

418 *C. alexandrinus* was slightly higher (0.013, $p = 0.028$) than that in the other direction
(0.010, $p = 0.028$). In *C. alexandrinus* populations, one likely migrant from *C. dealbatus*
420 and two hybrid F1 individuals were identified (probability higher than 0.5). With the
same threshold value, two migrants and one F1 individual were identified in *C.*
422 *dealbatus* populations.

424 **The detection of hybrid individuals**

Analyses with NewHybrids provided no evidence of a large number of hybrids or a
426 higher frequency of these near the potential contact area between the species. Based
on the STRUCTURE results and simulations, the optimal threshold for distinguishing
428 hybrids from non-hybrids was $q=0.836$. Based on this threshold, 81.9% of the
individuals (204 out of 246) collected from sites at the northern Chinese coastline,
430 Qinghai Lake and Taiwan Island were assigned to *C. alexandrinus* (Figure 2c-d).
Individuals with intermediate q-values, which were possibly hybrids, were found at
432 most northern Chinese sampling sites (Figure 2d). For the southern coastline in China,
145 out of 156 Individuals (92.9%) belonged to *C. dealbatus* with a probability larger
434 than 0.836 (Figure 2c-d). Only one individual of each species was assigned to the
genetic cluster representing the other species with high probability (Figure 2d).

436

The result of NewHybrids was highly concordant with STRUCTURE results and
438 suggested migrants moving in both directions. NewHybrids consistently identified
three migrants mentioned above with probability higher than 99%. However,
440 NewHybrids failed to identify simulated hybrid individuals and recognized them as
migrants. Thus, the result of NewHybrids was not used for hybrid identification (Fig
442 S3).

444 **Niche modeling, projections and comparisons**

Our ecological niche models effectively captured the current distribution of both *C.*
446 *alexandrinus* and *C. dealbatus* (Figure 4) with a high discrimination capacity (AUC
values > 0.88 for training and test data). Jackknife tests on variable importance for *C.*

448 *alexandrinus* revealed that isothermality, precipitation seasonality and mean
temperature of the warmest quarter were the three highest ranked variables when
450 used in isolation. For *C. dealbatus*, mean diurnal range and annual precipitation were
the most important variables. The simulation of the three periods, i.e. Last Interglacial
452 (LIG, 120-100Ka), Last Glacial Maximum (LGM, 21Ka, MIROC model) and current
times, respectively, showed range shifts in both species. In particular, these results
454 suggest that ranges of both species shrank during the LIG in the Chinese coastal area
accompanied by an increase of climatic suitability in the inland region for *C.*
456 *alexandrinus*. In contrast, suitable habitats expanded for both species during the LGM
in the coastal area, the East China Sea and the northern part of the South China Sea
458 (sea area between Hainan and Taiwan), probably due to the fall of the sea level.

460 The ordination approach using PCA-env suggested that the overlap of the current
climatic niches of the two species is relatively low (Figure S4a-b). The two species can
462 be separated based on the first two PCs with an accumulative 81.5% of the total
variance explained (Figure S4c). The niche equivalency test rejected the null
464 hypothesis that the species pair is distributed in identical environmental space ($p =$
0.019; Figure S4d).

466

Stable-isotope analysis

468 Our stable-isotope analysis showed that *C. dealbatus* exhibited significantly higher
 $\delta^{15}\text{N}$ values than *C. alexandrinus* ($p < 0.001$, Figure 5a, Figure S5). In contrast, we did
470 not find significant differences in $\delta^{13}\text{C}$ between the two species ($p = 0.161$). Further
isotope space overlap analysis showed that *C. alexandrinus* individuals had a high
472 probability to be found within the isotopic niche space of *C. dealbatus* (95.3%), while *C.*
dealbatus individuals showed a relatively low probability to be found in the isotopic
474 niche space of *C. alexandrinus* (46.5%, Figure 5b). Moreover, we found that *C.*
alexandrinus showed higher variability in $\delta^{15}\text{N}$ profile across breeding populations than
476 *C. dealbatus*.

478 **4 DISCUSSION**

Our genetic data show that *C. alexandrinus* and *C. dealbatus* have diverged to a level
480 of advanced sorting of alleles between the two species particularly in mtDNA and
Z-linked genes with lower effective population sizes (Figure 2a-b). For autosomal
482 microsatellite data, we also found that genetic differentiation is low at intraspecific level
but substantially high between the species (Figure 2c-d, Table 2). Though it is unclear
484 whether a narrow hybrid zone exists in the contact area on the Chinese coast, a
considerable level of symmetric gene flow occurred between the two plovers (Table 3).
486 We find diagnosable differences in morphometric traits and ecological characters
between the two plovers along the coast. At odds with these results, a previous work
488 found no evidence of genetic differentiation between the two plovers (Rheindt et al.
2011). The present dataset comprises of systematically sampling along the Chinese
490 coast, a larger suite of genetic markers and well-characterized ecological traits (Figure
1) while Rheindt et al. (2011) analyzed samples collected outside the breeding season.
492 Potentially erroneous species assignment of non-breeding birds may underestimate
genetic differentiation, because the distinguishing features in non-breeding plumage
494 are relatively subtle (Bakewell & Kennerley 2008; Kennerley et al. 2008; Rheindt et al.
2011) and non-breeding *C. alexandrinus* and *C. dealbatus* mix frequently on the coast
496 of the South China sea (own observation and Kennerley et al. 2008).

498 **Phylogeographic patterns in *C. alexandrinus* and *C. dealbatus***

Two genetic lineages were found among breeding *Charadrius* plovers along the
500 Chinese coast, corresponding the northern lineage to *C. alexandrinus* and the
southern one to *C. dealbatus*, respectively (Figure 1a, Table 2). The sharp genetic
502 break between the two lineages lies between Wenzhou and Fuzhou (latitude 26-27 °N)
north of the Taiwan Strait (Figure 2c-d). Furthermore, samples from Taiwan Island
504 belong to *C. alexandrinus* but the population in Jinmen Island is affiliated with *C.*
dealbatus (Figure 2c-d). This pattern likely reflects historical isolation of the two
506 species through separation by some geographical barriers at the Chinese coast during
the Pleistocene climatic fluctuation periods. Divergence between the two plovers
508 560,000 years ago was inferred based on IM for the two species (Table 3, Figure 3).

This period falls into the Marine Isotope Stage 16 of the mid-late Pleistocene, during
510 which was one of the Ice Age (Railsback et al. 2015). Accordingly the divergence
between the plovers was probably linked to vicariance when the coastline was
512 separated by a land-bridge raised due to the shallow sills between the East and the
South China Sea (Ni et al. 2014). *Charadrius* plovers have originated in the Northern
514 hemisphere and then radiated to the Southern hemisphere as suggested by a recent
molecular phylogeny (Dos Remedios et al. 2015). It is thereby likely that *C. dealbatus*
516 originated from *C. alexandrinus* and could have been diverging along the east China
coast since the mid-late Pleistocene.

518
Phylogeographic patterns have been relatively well characterized in shorebirds
520 breeding at high latitudes (Trimbos et al. 2011; Küpper et al. 2012; Miller et al. 2014).
Panmixia or weak genetic differentiation was usually suggested, most likely driven by
522 extensive gene flow. However, it seems that islands can act as a barrier to natal
dispersal for the continental Kentish plovers (Küpper et al. 2012). In contrast,
524 population structures in temperate and subtropical shorebird populations are poorly
documented, probably due to a low level of species diversity. To the best of our
526 knowledge, our study shows the first documented phylogeographic break in a bird
species in the coastline in China. Interestingly, concordant phylogeographic patterns
528 have been described in several coastal marine taxa, such as plants (Wang et al. 2015),
fishes (Ding et al. 2018; Liu et al. 2007), shellfishes (Ni et al. 2012), and crustaceans
530 (Wang et al. 2008). Though the exact splitting times are not congruent, the observed
split line is at approximately 25°N latitude between the East China Sea and the
532 Southern China Sea (reviewed in Ni et al. 2014). This consensus pattern resulted in
the hypothesis that historical factors, i.e. sea level fluctuation during the Pleistocene,
534 caused a convergent phylogeographic pattern in multiple coastal marine fauna in the
marginal northwestern Pacific Ocean (Ni et al. 2014; Ding et al. 2018). Thus, our study
536 contributes a vertebrate case to the accumulating literature about this species
divergence hotspot. Apart from the major role of physical barriers, comparative
538 phylogeographic studies also revealed that other abiotic factors, like ocean current and

hydrothermal conditions, as well as species ecological characters, i.e. dispersal ability, 540 habitat preference, life-history, and population demography can also play a role in contributing to divergence of coastline fauna (Liu et al. 2007; Ni et al. 2014).

542

Morphological and ecological differentiation along a latitudinal gradient

544 The two plovers, *C. alexandrinus* and *C. dealbatus* are distributed along the Chinese coastline across a latitudinal and associated environmental gradients from temperate 546 to tropical zones. Within each species, we found a general trend that northern populations have larger values than the southern counterparts in morphometry (Figure 548 1). This pattern may be related to Bergmann's rule which states that body size of homeothermic animals is larger in colder climates than in warmer ones (Bergmann 550 1848). Populations of both plover species distributed in such a north-south gradient may benefit from an optimal temperature control (Salewski & Watt 2017). A mutually 552 non-exclusive explanation is that the difference in morphological traits, i.e. body mass and bill length link to potential differences in resource exploitation and life history. Our 554 data show that *C. dealbatus* has a larger average body mass than *C. alexandrinus*. Body mass is a comprehensive trait reflecting nutrition assimilation, energy reservation 556 and expenditure (McNab 2009). The difference in body mass might be related to the difference in migration behavior where a lighter body mass in *C. alexandrinus* is 558 favored by decreased transport cost of fuel storage during migration (Alerstam et al. 2003; McWilliams & Karasov 2001). In contrast, larger body mass in *C. dealbatus*, a 560 short-distance migrant or resident, may be beneficial in multiple reproduction within a single breeding season while *C. alexandrinus* produces usually only a single clutch 562 (Lin et al. in prep.). Difference in bill length may be driven by the difference in the use of food resources (Badyaev et al. 2008) but recently, the function of the bill as 564 temperature regulator also started to attract scientific attention (Tattersall et al. 2016). On the other hand, an increasing number of studies have demonstrated that birds at 566 higher latitude and in cooler environments have shorter bills (e.g. European sparrows, Johnston 1969; Australian shorebirds, Nebel et al. 2013), consistent with Allen's Rule 568 (Allen 1877). Nevertheless, we find that populations of *C. alexandrinus* in Taiwan had

similarly large body mass and bill lengths as *C. dealbatus* populations (Figure 1b-d, g),
570 which are significantly larger than mainland conspecific populations. This is probably
caused by phenotypic plasticity in the Taiwan population to a sub-tropical ecology and
572 resident life history, similar to the populations of *C. dealbatus* in the South China sea
coast.

574

Climatic niche modelling indicates that the climatic conditions of the two species are
576 spatially separated (Figure S4). *C. dealbatus* is restricted to breeding sites close to the
coast, particularly in warmer tropical climate. In contrast, *C. alexandrinus* has a wider
578 climatic niche, as represented by a broader climatic zone (Figure 4). This species can
breed not only on temperate coasts (Que et al. 2015) but also in inland saline lake
580 shore (Cramp & Perrins 1983), just as Qinghai Lake. In addition, our isotope analysis
revealed that *C. alexandrinus* covered a wider range of isotope ratios than *C.*
582 *dealbatus*, but *C. alexandrinus* exploited a lower trophic range ($\delta^{15}\text{N}$). This indicates
that *C. dealbatus* probably feeds on a higher energy diet than its sister species
584 (Hobson & Clark 1992). However, it is unclear whether such difference may result from
diet preference divergence or due to differences in food resource availability
586 (McCormack et al. 2010). Taken together, these results suggest that the ecological
niches of the two plovers are significantly different in several aspects, and support a
588 role for ecology in constraining range limits and perhaps habitat preference for the two
shorebird species.

590

Incipient speciation with ongoing gene flow

592 We find evidence of incipient speciation with ongoing gene flow between the two
plovers. The IM results indicate a relatively young split with considerable gene flow
594 between the two species (Figure 3 and Table 3). We suggest this is probably due to
gene flow caused by secondary contact during the Pleistocene, because our niche
596 modeling analysis reveals that the ranges of the two species were expanded and
consequently overlapped between the Eastern and Southern China Sea during the
598 Last Glacial Maximum (Figure 4). While our niche modeling demonstrates a cycle of

range dynamics caused by sea-level changes, one should bear in mind that the last
600 million years witnessed multiple glaciation cycles (Taylor et al. 2014, 2015). In
particular, marine oxygen isotope records designate 28 isotope stages corresponding
602 to glacio-climatic cycles in the last million years (Railsback et al. 2015). For ocean
marginal and coastline taxa, this may imply that the fluctuations in sea level can lead to
604 alternation between population isolation and contact throughout their evolutionary
histories. This can in turn yield significant consequences on population divergence and
606 historical demography because speciation can proceed through cycles of allopatric
stages interspersed by parapatry, resulting in a diversification process characterized
608 by isolation with migration (Rheindt & Edwards, 2011).

610 Under this premise, a key question arises: after the two plovers diverged, how was
their divergence maintained in the presence of ongoing gene flow? Speciation theory
612 predicts that divergence is initiated either by genetic drift or divergent selection (Lynch
et al. 2016; Rundle & Nosil 2005; Seehausen et al. 2014; Wolf & Ellegren 2017).
614 However, genetic drift is unlikely to have been the only force to initiate divergence in
the plovers for two reasons: the large effective population sizes (Ne) and a relatively
616 high level of gene flow (Table 3). Moreover, large Ne and recent divergence make it
unlikely that genetic drift could have led to diagnosable differences between
618 populations (Ellstrand & Elam 1993; Lanfear et al. 2014), and gene flow directly
counteracts the diverging effects of drift (García-Navas et al. 2015; Poelstra et al.
620 2014). Another possibility is that sufficient divergent selection could contribute to
overcome the homogenizing effects of gene flow (Coyne & Orr 2004; Feder et al. 2013;
622 Nosil & Feder 2012; Wagner et al. 2012; Wolf & Ellegren 2017). In light of this view, the
“genomic islands of speciation” model was proposed to illustrate that divergent
624 selection can have effects in specific regions across the genome leading to divergence
with gene flow (Feder et al. 2013; Nosil & Feder 2012; Wagner et al. 2012; Wolf &
626 Ellegren 2017). Data from several organisms suggest that incipient speciation can be
maintained with divergence at a small number genomic regions (Martin et al. 2013;

628 Morales et al. 2017; Nadachowska-Brzyska et al. 2013; Towes et al. 2016 but see
Curickshan et al. 2014, Burri 2017).

630

The geographical boundary between the two plovers was ambiguously defined in
632 previous studies (Kennerley et al. 2008; Rheindt et al. 2011). Our results show that the
discontinuity in genetic structuring (Figure 2c) and morphometric values (Figure 1b-d)
634 between the two species is situated at coastline between Wenzhou and Fuzhou,
indicating a contact zone (Figure 2c). For incipient species, individuals may show a
636 clinal pattern of allele frequency and morphology at their contact and form a hybrid
zone (Bastos□Silveira et al. 2012; Harrison 1986; Taylor et al. 2014). Our
638 STRUCTURE results revealed no obvious signs of a hybrid zone (Figure 2d), and
rather indicated sporadic migrants in the respective range of the other species. One
640 possibility is that our sampling transect was not fine-grained enough to be able to
discover the potential hybrid zone, which would thus be narrower than the 200 km
642 distance between the two neighboring sampling sites. Another possibility for an
apparent lack of a hybrid zone is assortative mating between the two plovers at the
644 contact (Bearhop et al. 2005). The latter explanation is supported by the fact that
populations of the two species close to this region were much more divergent in
646 morphological traits than ones farther apart (Figure 1b-d). Reproductive character
displacement between the two species (Brown & Wilson 1956; Robinson & Wilson
648 1994; Grant and Grant 2006) in the contact regions would constrain interbreeding
(Rybinski et al. 2016; Winkelmann et al. 2014). Obviously, genetic data alone cannot
650 demonstrate this and detailed experiments related to assortative mating in the contact
zone are required.

652

Taxonomic implications

654 This study offers several taxonomic implications for the *C. alexandrinus* complex in
East Asia. Kennerley et al. (2008) recommended that the tropical breeding population,
656 previously defined as the subspecies *dealbatus* warranted species status, based on
differentiation in morphology, behavior and distribution from *C. alexandrinus*.

658 Uncertainty arose about the taxonomic status because *dealbatus* was not
distinguished from *C. alexandrinus* in a first genetic evaluation (Rheindt et al. 2011).
660 Our results provide further support for a pair of incipient species, indicating that *C.*
dealbatus is the youngest species within the genus *Charadrius* (Barth et al. 2013).
662 Although we did not apply explicit Bayesian species delimitation analyses (e.g. Yang &
Rannala 2014), our results clearly demonstrate multiple diagnosable morphological
664 characters and distinct ecological niches, which are likely key factors to maintain
species limits. Beyond the detection of differences between these plovers, this study
666 forms a basis for conservation considerations of *C. dealbatus* because of its restricted
range and adaptation to subtropical climate, as well as a risk of population decline
668 caused by habitat loss in the China coastline (Ma et al. 2014).

670 **Conclusions and perspectives**

Resolving the balance between diverging selection and gene flow is of fundamental
672 importance to understand speciation processes. Here, we show that *C. alexandrinus*
and *C. dealbatus* represent a case of incipient species in which divergent selection
674 associated with ecological differences likely works as efficient mechanism for the
maintenance of divergence in the face of gene flow. While the full species status of *C.*
676 *dealbatus* may be justified, it remains untested whether a strong level of reproductive
isolation has been established between *C. alexandrinus* and *C. dealbatus*. Further, we
678 have shown low genetic divergence between the two plovers, so it would be of
particular importance to explore the patterns of divergence at the genome level and
680 determine whether specific regions are related reproductive isolation and adaptation.
In addition, the IM analysis presented here estimated average historical gene flow, but
682 it would be interesting to evaluate more realistic (and complex) demographic models in
order to estimate changes in N_e and the span of isolation and secondary contact better.
684 Genome-wide population genetic approaches promise the power for better resolved
evolutionary history of the two *Charadrius* plovers but also open an avenue to
686 characterize the genetic architecture associated with phenotypic trait divergence and

local adaptation (Freedman et al. 2014; Nadachowska-Brzyska et al. 2013; Towes et al.
688 2016).

690 **ACKNOWLEDEMENTS**

We thank Qiaoyi Liang, Xiaoyan Long, Derong Meng, Demeng Jiang, Li Tian and Hebo
692 Peng help with field sampling, Guoling Chen, Yangkai Zhou for their assistance with
laboratory works. Special thanks are due Shaochong Peng for preparing sketches of
694 plovers in Figure 1.

696 **Funding information:**

This study was supported by National Natural Science Foundation of China,
698 Grant/Award Number: 31301875 and 31572251 to YL, 31600297 to PJQ and
31572288 to ZWZ; and the Open Grant of the State Key Laboratory of Biocontrol of
700 Sun Yat-sen University to YL and TZ (SKLBC13KF03), Youth Innovation Promotion
Association CAS (2015304) to JHH. Computational machinery time work was granted
702 by Special Program for Applied Research on Super Computation of the
NSFC-Guangdong Joint Fund (the second phase) under Grant No. U1501501 to YL.

704

DATA ACCESSIBILITY

706 Sequences deposited at GenBank: accession number xxxx-xxxxx
Phenotype, distribution, stable isotope and microsatellite genotypes available at:
708 Dryad Doi: xxx

710 **AUTHOR CONTRIBUTIONS**

Y.L., Z.W.Z. and T. S. conceived and designed the study, P.J.Q., C-Y.C., Q.H., J.M.,
712 N.Z., X.J.W., and T. S. collected data in the field, X.J.W. and S.M.L conducted
molecular genetic laboratory work, X.J.W. P.J.Q. analyzed genetic data with input from
714 Y.L. and G.H.. J.H.H. performed niche modeling analysis, C.C.Z. carried out stable
isotope analysis with input from E.P.-G. and C.D.. X.J.W P.J.Q. and Y.L. wrote the

716 manuscript with input from J.H.H., G.H., X.C.Z. and C.D. All authors gave final
717 approval for publication.

718

REFERENCES

720 Alerstam T, Hedenstrom A and Åkesson S (2003) Long-distance migration: evolution and determinants.
Oikos, **103**, 247-260.

722 Allen JA (1877) The influence of physical conditions in the genesis of species. *Radical Review* **1**,
108-140.

724 Anderson E, Thompson E (2002) A model-based method for identifying species hybrids using
multilocus genetic data. *Genetics* **160**, 1217-1229.

726 Arguedas N, Parker PG (2000) Seasonal migration and genetic population structure in house wrens.
The Condor **102**, 517-528.

728 Badyaev AV, Young RL, Oh KP, Addison C (2008) Evolution on a local scale: developmental, functional,
and genetic bases of divergence in bill form and associated changes in song structure
730 between adjacent habitats. *Evolution* **62**, 1951-1964.

732 Bakewell D, Kennerley P (2008) Field characteristics and distribution of an overlooked Charadrius
plover from South-East Asia. *Birding Asia* **9**, 46-57.

734 Bandelt H-J, Forster P, Röhl A (1999) Median-joining networks for inferring intraspecific phylogenies.
Molecular Biology and Evolution **16**, 37-48.

736 Barth JM, Matschiner M, Robertson BC (2013) Phylogenetic position and subspecies divergence of the
738 endangered New Zealand Dotterel (*Charadrius obscurus*). *PLoS ONE* **8**, e78068.

Bearhop S, Fiedler W, Furness RW, *et al.* (2005) Assortative mating as a mechanism for rapid evolution
738 of a migratory divide. *Science* **310**, 502-504.

740 Beaumont MA, Zhang W, Balding DJ (2002) Approximate Bayesian computation in population genetics.
Genetics **162**, 2025-2035.

Bergmann C (1848) *Über die Verhältnisse der Wärmeökonomie der Thiere zu ihrer Grösse*.

742 Bernardi G, Alva-Campbell YR, Gasparini JL, Floeter SR (2008) Molecular ecology, speciation, and
744 evolution of the reef fish genus *Anisotremus*. *Molecular Phylogenetics and Evolution* **48**,
929-935.

746 Broennimann O, Fitzpatrick MC, Pearman PB, *et al.* (2012) Measuring ecological niche overlap from
occurrence and spatial environmental data. *Global Ecology and Biogeography* **21**, 481-497.

Brown WL, Wilson EO (1956) Character displacement. *Systematic Zoology* **5**, 49-64.

748 Bruen TC, Philippe H, Bryant D (2006) A simple and robust statistical test for detecting the presence of
recombination. *Genetics* **172**, 2665-2681.

750 Burri R (2017) Linked selection, demography and the evolution of correlated genomic landscapes in
birds and beyond. *Molecular Ecology* **26**, 3853-3856.

752 Carson H, Clague D (1995) Geology and biogeography of the Hawaiian Islands. *Hawaiian Biogeography:
Evolution on a Hot Spot Archipelago*, 14-29.

754 Chapuis M-P, Estoup A (2007) Microsatellite null alleles and estimation of population differentiation.
Molecular Biology and Evolution **24**, 621-631.

756 Chen Q, Liu Y, Ho WT, Chan SK, Li QH, & Huang JR (2017) Use of stable isotopes to understand food
webs in Macao wetlands. *Wetlands Ecology and Management* **25**, 59-66.

758 Coyne JA, Orr HA (2004) *Speciation* Sinauer Associates Sunderland, MA.

760 Cramp S, Perrins C (1983) The Birds of Europe the Middle East and North Africa, Vol. III (Waders to Gulls). *Oxford University Press, Oxford.* pp 153-166.

762 Cruickshank TE, Hahn MW. (2014) Reanalysis suggests that genomic islands of speciation are due to reduced diversity, not reduced gene flow. *Molecular Ecology* **23**,3133-3157.

764 del Hoyo J, Collar N, Kirwan GMS, C.J. (2016) *White-faced Plover (Charadrius dealbatus)*. In: *del Hoyo, J., Elliott, A., Sargatal, J., Christie, D.A. & de Juana, E. (eds.). Handbook of the Birds of the World Alive. Lynx Edicions, Barcelona.*, retrieved from <http://www.hbw.com/node/467300> on 16 June 2018

766 DeNiro MJ, Epstein S (1978) Carbon isotopic evidence for different feeding patterns in two hyrax species occupying the same habitat. *Science* **201**, 906-908.

768 Ding S, Mishra M, Wu H, et al (2018) Characterization of hybridization within a secondary contact region of the inshore fish, *Bostrychus sinensis*, in the East China Sea. *Heredity*, **120**, 51-62.

770 Dos Remedios N, Lee PL, Burke T, Székely T, Küpper C (2015) North or south? Phylogenetic and 772 biogeographic origins of a globally distributed avian clade. *Molecular Phylogenetics and Evolution* **89**, 151-159.

774 Earl DA (2012) STRUCTURE HARVESTER: a website and program for visualizing STRUCTURE output and implementing the Evanno method. *Conservation Genetics Resources* **4**, 359-361.

776 Eberhart-Phillips LJ, Hoffman JI, Brede EG, et al. (2015) Contrasting genetic diversity and population structure among three sympatric Madagascan shorebirds: parallels with rarity, endemism, 778 and dispersal. *Ecology and Evolution* **5**, 997-1010.

780 Ellstrand NC, Elam DR (1993) Population genetic consequences of small population size: implications for plant conservation. *Annual Review of Ecology and Systematics* **24**, 217-242.

782 Evanno G, Regnaut S, Goudet J (2005) Detecting the number of clusters of individuals using the software STRUCTURE: a simulation study. *Molecular Ecology* **14**, 2611-2620.

784 Excoffier L, Laval G, Schneider S (2005) Arlequin (version 3.0): An integrated software package for 786 population genetics data analysis. *Evolutionary Bioinformatics* **1**, 47-50.

Feder JL, Flaxman SM, Egan SP, Comeault AA, Nosil P (2013) Geographic mode of speciation and 788 genomic divergence. *Annual Review of Ecology, Evolution, and Systematics* **44**, 73-97.

Fitzpatrick SW, Gerberich JC, Kronenberger JA, Angeloni LM, Funk WC (2015) Locally adapted traits 790 maintained in the face of high gene flow. *Ecology Letters* **18**, 37-47.

Freedman AH, Gronau I, Schweizer RM, et al. (2014) Genome sequencing highlights the dynamic early 792 history of dogs. *PLoS Genetics* **10**, e1004016.

Funk WC, Mullins TD, Haig SM (2007) Conservation genetics of snowy plovers (*Charadrius alexandrinus*) 794 in the Western Hemisphere: population genetic structure and delineation of subspecies. *Conservation Genetics* **8**, 1287-1309.

García-Navas V, Bonnet T, Waldvogel D, et al. (2015) Gene flow counteracts the effect of drift in a 796 Swiss population of snow voles fluctuating in size. *Biological Conservation* **191**, 168-177.

Ginn H, Melville D (1983) Moulting in birds. BTO Guide 19. *British Trust for Ornithology, Tring.*

Grant PR, Grant BR (2006). Evolution of character displacement in Darwin's finches. *Science* **313**, 798 224-226.

Guillot G, Mortier F, Estoup A (2005) GENELAND: a computer package for landscape genetics. 800 *Molecular Ecology Notes* **5**, 712-715.

Hammer Ø, Harper D, Ryan P (2001) PAST: Paleontological Statistics Software Package for education

802 and data analysis. *Palaeontolia Electronica* 4.

804 Harrison RG (1986) Pattern and process in a narrow hybrid zone. *Heredity* **56**, 337.

806 Hartert E, Jackson AC (1915) Notes on some waders. *Ibis* **57**, 526-534.

808 Hey, J. (2006). Recent advances in assessing gene flow between diverging populations and species. *Current Opinion in Genetics & Development* **16**, 592-596.

810 Hey J (2010) Isolation with migration models for more than two populations. *Molecular Biology and Evolution* **27**, 905-920.

812 Hey J, Nielsen R (2004) Multilocus methods for estimating population sizes, migration rates and divergence time, with applications to the divergence of *Drosophila pseudoobscura* and *D. persimilis*. *Genetics* **167**, 747-760.

814 Hey J, Nielsen R (2007) Integration within the Felsenstein equation for improved Markov chain Monte Carlo methods in population genetics. *Proceedings of the National Academy of Sciences of the United States of America* **104**, 2785-2790.

816 Hijmans RJ, Cameron SE, Parra JL, Jones PG, Jarvis A (2005) Very high resolution interpolated climate surfaces for global land areas. *International Journal of Climatology* **25**, 1965-1978.

818 Hobson KA, Clark RG (1992) Assessing avian diets using stable isotopes I: turnover of ^{13}C in tissues. *Condor* **94**, 181-188.

820 Hoskin CJ, Higgle M (2010) Speciation via species interactions: the divergence of mating traits within species. *Ecology Letters* **13**, 409-420.

822 Hu J, Broennimann O, Guisan A, et al. (2016) Niche conservatism in *Gynandropaa* frogs on the southeastern Qinghai-Tibetan Plateau. *Scientific Reports* **6**, 32624.

824 Hubisz MJ, Falush D, Stephens M, Pritchard JK (2009) Inferring weak population structure with the assistance of sample group information. *Molecular Ecology Resources* **9**, 1322-1332.

826 BirdLife International (2016) *IUCN Red List for birds*. Downloaded from <http://www.birdlife.org> on 8/09/2016.

828 Jackson DU, dos Remedios N, Maher KH, et al. (2017) Polygamy slows down population divergence in shorebirds. *Evolution* **71**, 1313-1326.

830 Jakobsson M, Rosenberg NA (2007) CLUMPP: a cluster matching and permutation program for dealing with label switching and multimodality in analysis of population structure. *Bioinformatics* **23**, 1801-1806.

832 Johnston RF (1969) Character variation and adaptation in European sparrows. *Systematic Biology* **18**, 206-231.

834 Küpper C, Edwards SV, Kosztolanyi A, et al. (2012) High gene flow on a continental scale in the polyandrous Kentish plover *Charadrius alexandrinus*. *Molecular Ecology* **21**, 5864-5879.

836 Küpper C, Horsburgh GJ, Dawson DA, et al. (2007) Characterization of 36 polymorphic microsatellite loci in the Kentish plover (*Charadrius alexandrinus*) including two sex-linked loci and their amplification in four other *Charadrius* species. *Molecular Ecology Notes* **7**, 35-39.

838 Kempenaers B, Valcu M (2017) Breeding site sampling across the Arctic by individual males of a polygynous shorebird. *Nature* **541**, 528.

840 Kennerley PR, Bakewell DN, Round PD (2008) Rediscovery of a long-lost Charadrius plover from South-East Asia. *Forktail* **24**, 63-79.

842 Lande R (1982) Rapid origin of sexual isolation and character divergence in a cline. *Evolution* **36**, 213-223.

844 Lanfear R, Kokko H, Eyre-Walker A (2014) Population size and the rate of evolution. *Trends in Ecology and Evolution* **29**, 62-69.

846 & *Evolution* **29**, 33-41.

848 Le Moan A, Gagnaire PA, Bonhomme F (2016) Parallel genetic divergence among coastal-marine
ecotype pairs of European anchovy explained by differential introgression after secondary
contact. *Molecular Ecology* **25**, 3187-3202.

850 Leigh JW, Bryant D (2015) Popart: full-feature software for haplotype network construction. *Methods*
in Ecology and Evolution **6**, 1110-1116.

852 Li JW, Yeung CK, Tsai P-W, et al. (2010) Rejecting strictly allopatric speciation on a continental island:
prolonged postdivergence gene flow between Taiwan (*Leucodopteron taewanus*,
Passeriformes Timaliidae) and Chinese (*L. canorum canorum*) hwameis. *Molecular Ecology* **19**,
494-507.

854 Liu JX, Gao TX, Wu SF, Zhang YP (2007) Pleistocene isolation in the Northwestern Pacific marginal seas
and limited dispersal in a marine fish, *Chelon haematocheilus* (Temminck & Schlegel, 1845).
Molecular Ecology **16**, 275–288.

856 Liu Y, Keller I, Heckel G. (2012). Breeding site fidelity and winter admixture in a long-distance migrant,
the tufted duck (*Aythya fuligula*). *Heredity*, **109**, 108-116.

858 Liu Y, Liu S, Yeh CF, Zhang N, Chen G, Que P, ... & Li SH. (2018). The first set of universal nuclear
860 protein-coding loci markers for avian phylogenetic and population genetic studies. bioRxiv,
272732.

862 Librado P, Rozas J (2009) DnaSP v5: a software for comprehensive analysis of DNA polymorphism data.
Bioinformatics **25**, 1451-1452.

864 Lynch M, Ackerman MS, Gout J-F, et al. (2016) Genetic drift, selection and the evolution of the
mutation rate. *Nature Reviews Genetics* **17**, 704-714.

866 Ma Z, Melville D S, Liu J, et al. (2014) Rethinking China's new great wall : Massive seawall construction
in coastal wetlands threatens biodiversity. *Science*, **346**, 912-914.

868 Martin SH, Dasmahapatra KK, Nadeau NJ, et al. (2013) Genome-wide evidence for speciation with
gene flow in *Heliconius* butterflies. *Genome Research* **23**, 1817-1828.

870 Mayr E (1963) *Animal species and evolution* Belknap Press of Harvard University Press Cambridge,
Massachusetts.

872 McCormack JE, Zellmer AJ, Knowles LL (2010) Does niche divergence accompany allopatric divergence
in *Aphelocoma* jays as predicted under ecological speciation?: insights from tests with niche
models. *Evolution* **64**, 1231-1244.

874 McNab BK (2009) Ecological factors affect the level and scaling of avian BMR. *Comparative
Biochemistry and Physiology Part A: Molecular & Integrative Physiology* **152**, 22-45.

876 McWilliams SR, Karasov WH (2001) Phenotypic flexibility in digestive system structure and function in
migratory birds and its ecological significance. *Comparative Biochemistry and Physiology Part
A: Molecular & Integrative Physiology* **128**, 577-591.

878 Miller MP, Haig SM, Mullins TD, Ruan L, et al. (2015) Intercontinental genetic structure and gene flow
in Dunlin (*Calidris alpina*), a potential vector of avian influenza. *Evolutionary Applications*, **8**,
149-171.

880 Morales AE, Jackson ND, Dewey TA, O'Meara BC, Carstens BC (2017) Speciation with gene flow in
North American *Myotis* bats. *Systematic Biology* **66**, 440-452.

882 Nadachowska-Brzyska K, Burri R, Olason PI, et al. (2013) Demographic divergence history of pied
flycatcher and collared flycatcher inferred from whole-genome re-sequencing data. *PLoS*

890 *Genetics* **9**, e1003942.

890 Nadeau NJ, Whibley A, Jones RT, *et al.* (2012) Genomic islands of divergence in hybridizing *Heliconius* butterflies identified by large-scale targeted sequencing. *Phil. Trans. R. Soc. B* **367**, 343-353.

892 Nebel S, Rogers KG, Minton CD, Rogers DI (2013) Is geographical variation in the size of Australian shorebirds consistent with hypotheses on differential migration? *Emu* **113**, 99-111.

894 Ni G, Li Q, Kong LF, Zheng XD (2012) Phylogeography of bivalve *Cyclina sinensis*: testing the historical glaciations and Changjiang River outflow hypotheses in northwestern Pacific. *PLoS ONE* **7**, e49487.

898 Ni G, Li Q, Kong LF & Yu Hong (2014) Comparative phylogeography in marginal seas of the northwestern Pacific, *Molecular Ecology*, **23**, 534-548.

900 Nielsen EE, Bach LA, Kotlicki P (2006) HYBRIDLAB (version 1.0): a program for generating simulated hybrids from population samples. *Molecular Ecology Notes* **6**, 971-973.

902 Nosil P (2007) Divergent host plant adaptation and reproductive isolation between ecotypes of *Timema cristinae* walking sticks. *The American Naturalist* **169**, 151-162.

904 Nosil P, Feder JL (2012) Genomic divergence during speciation: causes and consequences. *Phil. Trans. R. Soc. B*, **367**, 332-342.

906 Nosil P, Schlüter D (2011) The genes underlying the process of speciation. *Trends in Ecology & Evolution* **26**, 160-167.

908 Pagani-Núñez E, Renom M, Mateos-Gonzalez F, Cotín J, Senar JC (2017) The diet of great tit nestlings: Comparing observation records and stable isotope analyses. *Basic and Applied Ecology* **18**, 57-66.

910 Peakall R, Smouse PE (2012) GenAIEx 6.5: genetic analysis in Excel. Population genetic software for teaching and research--an update. *Bioinformatics* **28**, 2537-2539.

912 Peters JL, McCracken KG, Pruett CL, *et al.* (2012) A parapatric propensity for breeding precludes the completion of speciation in common teal (*Anas crecca*, *sensu lato*). *Molecular Ecology* **21**, 4563-4577.

914 Phillips SJ, Dudik M, Elith J, *et al.* (2009) Sample selection bias and presence-only distribution models: implications for background and pseudo-absence data. *Ecological Applications* **19**, 181-197.

916 Poelstra JW, Vijay N, Bossu CM, *et al.* (2014) The genomic landscape underlying phenotypic integrity in the face of gene flow in crows. *Science* **344**, 1410-1414.

918 Primmer C, Møller A, Ellegren H (1995) Resolving genetic relationships with microsatellite markers: a parentage testing system for the swallow *Hirundo rustica*. *Molecular Ecology* **4**, 493-498.

920 Pritchard JK, Stephens M, Donnelly P (2000) Inference of population structure using multilocus genotype data. *Genetics* **155**, 945-959.

922 Procházka P, Stokke BG, Jensen H, *et al.* (2011) Low genetic differentiation among reed warbler *Acrocephalus scirpaceus* populations across Europe. *Journal of Avian Biology* **42**, 103-113.

924 Que P, Chang Y, Eberhart-Phillips L, *et al.* (2015) Low nest survival of a breeding shorebird in Bohai Bay, China. *Journal of Ornithology* **156**, 297-307.

926 R Development Core Team (2013) *R: a language and environment for statistical computing*. R Foundation for Statistical Computing, , Vienna, Austria. <http://www.r-project.org/>

928 Railsback LB, Gibbard PL, Head MJ, Voarintsoa NRG, Toucanne S (2015) An optimized scheme of lettered marine isotope substages for the last 1.0 million years, and the climatostratigraphic nature of isotope stages and substages. *Quaternary Science Reviews* **111**, 94–106.

932 Redfern CP, Clark JA (2001) Ringers' Manual. British Trust for Ornithology.

934 Rheindt FE, Edwards SV (2011) Genetic introgression: an integral but neglected component of
speciation in birds. *Auk* **128**:620–632

936 Rheindt FE, Székely T, Edwards SV, *et al.* (2011) Conflict between genetic and phenotypic
differentiation: the evolutionary history of a 'lost and rediscovered' shorebird. *PLoS ONE* **6**,
e26995.

938 Robinson BW, Wilson DS (1994) Character release and displacement in fishes: a neglected literature.
The American Naturalist **144**, 596–627.

940 Rundle HD, Nosil P (2005) Ecological speciation. *Ecology Letters* **8**, 336–352.

942 Rybinski J, Sirkiä PM, McFarlane SE, *et al.* (2016) Competition driven buildup of habitat isolation and
selection favoring modified dispersal patterns in a young avian hybrid zone. *Evolution* **70**,
2226–2238.

944 Salewski V, Watt C (2017) Bergmann's rule: a biophysiological rule examined in birds. *Oikos* **126**.

946 Schlüter D (2009) Evidence for ecological speciation and its alternative. *Science* **323**, 737–741.

948 Seehausen O, Butlin RK, Keller I, *et al.* (2014) Genomics and the origin of species. *Nature Reviews
Genetics* **15**, 176–192.

950 Sethuraman A, Hey J (2016) IMa2p-parallel MCMC and inference of ancient demography under the
Isolation with migration (IM) model. *Molecular Ecology Resources* **16**, 206–215.

952 Slatkin M (1973) Gene flow and selection in a cline. *Genetics* **75**, 733–756.

954 Stephens M, Donnelly P (2003) A comparison of bayesian methods for haplotype reconstruction from
population genotype data. *American Journal of Human Genetics* **73**, 1162–1169.

956 Stephens M, Smith NJ, Donnelly P (2001) A new statistical method for haplotype reconstruction from
population data. *The American Journal of Human Genetics* **68**, 978–989.

958 Storz JF (2002) Contrasting patterns of divergence in quantitative traits and neutral DNA markers:
analysis of clinal variation. *Molecular Ecology* **11**, 2537–2551.

960 Swanson HK, Lysy M, Power M, *et al.* (2015) A new probabilistic method for quantifying n-dimensional
ecological niches and niche overlap. *Ecology* **96**, 318–324.

962 Swinhoe R (1870) On the plovers of the genus *Aegialites* found in China. *Proceedings of the Zoological
Society London* **1870**, 136–142.

964 Székely T, Kosztolányi A, Küpper C (2008) Practical guide for investigating breeding ecology of Kentish
plover. (available at
http://www.bath.ac.uk/bio-sci/biodiversity-lab/pdfs/KP_Field_Guide_v3.pdf).

966 Tajima F (1989) Statistical method for testing the neutral mutation hypothesis by DNA polymorphism.
Genetics **123**, 585–595.

968 Tamura K, Stecher G, Peterson D, Filipski A, Kumar S (2013) MEGA6: Molecular Evolutionary Genetics
Analysis version 6.0. *Molecular Biology and Evolution* **30**, 2725–2729.

970 Tattersall GJ, Arnaout B, Symonds MR (2016) The evolution of the avian bill as a thermoregulatory
organ. *Biological Reviews* **92**, 1630–1652.

972 Taylor SA, White TA, Hochachka WM, *et al.* (2014) Climate-mediated movement of an avian hybrid
zone. *Current Biology* **24**, 671–676.

974 Taylor SA, Larson EL, Harrison RG (2015) Hybrid zones: windows on climate change. *Trends in Ecology
and Evolution* **30**, 398–406.

974 Trimbos K B, Musters C J M, Verkuil Y I, *et al.* (2011) No evident spatial genetic structuring in the
rapidly declining Black-tailed Godwit *Limosa limosa*, in The Netherlands. *Conservation*

976 *Genetics* **12**, 629-636.

978 Toews DPL, Taylor SA, Vallender R, Brelsford A, Butcher BG, Messer PW, Lovette IJ. (2016) Plumage
 genes and little else distinguish the genomes of hybridizing warblers. *Current Biology* **26**,
 2313–2318.

980 Vähä J, Primmer C (2006) Efficiency of model-based Bayesian methods for detecting hybrid
 individuals under different hybridization scenarios and with different numbers of loci.
982 *Molecular Ecology* **15**, 63-72.

984 Wagner CE, Harmon LJ, Seehausen O (2012) Ecological opportunity and sexual selection together
 predict adaptive radiation. *Nature* **487**, 366-369.

986 Wang C, Li C, & Li S. (2008) Mitochondrial DNA-inferred population structure and demographic history
 of the mitten crab (*Eriocheir* sensu *stricto*) found along the coast of mainland
 China. *Molecular Ecology* **17**, 3515-3527.

988 Wang J, Tsang LM, Dong YW (2015) Causations of phylogeographic barrier of some rocky shore species
 along the Chinese coastline. *BMC Evolutionary Biology* **15**, 114.

990 Weir JT, & Schlüter D. (2008). Calibrating the avian molecular clock. *Molecular Ecology*, **17**, 2321-2328.

992 Winkelmann K, Genner MJ, Takahashi T, Rüber L (2014) Competition-driven speciation in cichlid fish.
 Nature Communications **5**, 3412.

994 Winker K, McCracken KG, Gibson DD, Peters JL (2013) Heteropatric speciation in a duck, *Anas crecca*.
 Molecular Ecology **22**, 5922-5935.

996 Wolf JB, Ellegren H (2017) Making sense of genomic islands of differentiation in light of speciation.
 Nature Reviews Genetics **18**, 87.

998 Won YJ, Hey J (2005) Divergence population genetics of chimpanzees. *Molecular Biology and Evolution*
 22, 297-307.

1000 Yang Z, Rannala B. (2014) Unguided species delimitation using DNA sequence data from multiple
 loci. *Molecular Biology and Evolution* **31**, 3125-3135.

1002 Zhang G, Li C, Li Q, *et al.* (2014) Comparative genomics reveals insights into avian genome evolution
 and adaptation. *Science* **346**, 1311-1320.

1004 Zhou Y, Duvaux L, Ren G, *et al.* (2016) Importance of incomplete lineage sorting and introgression in
 the origin of shared genetic variation between two closely related pines with overlapping
 distributions. *Heredity* **118**, 211-220.

1006

1008 **FIGURE LEGENDS**

1010 **FIGURE 1** Sampling localities, morphology and trophic level differentiation of the
Kentish Plover *Charadrius alexandrinus* (blue) and the White-faced Plover *C. dealbatus* (yellow).

1012 **(a)** Samples were from an inland site (1, Qinghai Lake), 16 Chinese mainland coastal
1014 localities (2, Tangshan; 3, Cangzhou; 4, Weifang; 5, Lianyungang; 6, Nantong; 7,
Ningbo; 8, Zhoushan; 9, Wenzhou; 12, Fuzhou; 13, Xiamen; 14, Jinmen; 15, Shanwei;
1016 16, Yangjiang; 17, Zhanjiang; 18, Beihai and 19, Dongfang), and two localities on
Taiwan Island (10, Xinbei and 11, Zhanghua).

1018 **(b-f)** Differences between two species in several characters. *C. alexandrinus* has on
average shorter bill length (except for Taiwan populations) **(b)**, wing length **(c)** and
1020 lower body mass (except for Taiwan populations) **(d)** than *C. dealbatus*. Localities with
less than five measured adults were excluded in these analyses. **(f)** Plots of the first
1022 two principal components and their associated variance explained which showed the
subtle morphometric differences between the two species. **(e)** *C. alexandrinus* has
1024 overall more darkish plumage than *C. dealbatus* and males of the latter species have
less black tinged on face and neck during breeding season. **(g)** Pairwise morphological
1026 difference Q_{ST} plotted against geographical distance between coastal populations of *C.*
alexandrinus and *C. dealbatus*. Q_{ST} values within species were marked by blue or
1028 yellow dots. Q_{ST} between species (grey circles) declined as the distance increased
(regression showed as the dashed line).

1030

1032 **FIGURE 2** Haplotype networks based on mitochondrial and nuclear DNA sequences,
and population genetic structures based on microsatellite loci. *C. alexandrinus* marked
in blue and *C. dealbatus* in yellow. **(a)** Haplotype networks of three mitochondrial loci.
1034 For ATPase6/8 and ND3, over 95% of the individuals are sorted into two major
haplogroups. **(b)** Examples of haplotype networks based on 55 to 80 individuals of four
1036 exonic nuclear loci. **(c)** Genetic clustering inferred with Geneland based on
microsatellite genotypes. Blue and yellow show the assignment probability of a

1038 location for alternative genetic clusters. Location numbers are consistent with Figure 1.

(d) Genetic clustering inferred with STRUCTURE using microsatellites.

1040

FIGURE 3 Posterior densities of population demographic parameters estimated using

1042 the isolation-with-migration model (IM) implemented in IMa2p. These analyses used
the combined data set of three mitochondrial (1729 bp) and 15 nuclear exonic loci

1044 (11209 bp). K represents the Kentish Plover *C. alexandrinus*; W represents

White-faced Plover *C. dealbatus*. (a) Population divergence times (T) of *C.*

1046 *alexandrinus* and *C. dealbatus*. (b) Population migration rates ($2NM$) stand for the
average number of individuals in each group that were migrants from the other group in

1048 the past. Gene flow on both directions was significant. (c) Effective population sizes
(N_e) of the two species and their most recent common ancestor.

1050

FIGURE 4 Predicted environmental suitability for *C. alexandrinus* (left) and *C.*

1052 *dealbatus* (right), via ecological niche modeling (ENM). ENM results are shown for the
Last Interglacial (LIG, 120-100Ka), Last Glacial Maximum (LGM, 21Ka, MIROC model)

1054 and current times, respectively.

1056 **FIGURE 5 (a)** Raw data (bottom-left), density distribution (top-left and bottom-right),

and stable isotope related to dietary niche regions (top right) of $\delta^{13}\text{C}$ and $\delta^{15}\text{N}$ of *C.*

1058 *alexandrinus* and *C. dealbatus* feathers generated by “nicheROVER” (Swanson *et al.*

2015). The niche region of *C. alexandrinus* (blue) was broader than and contained

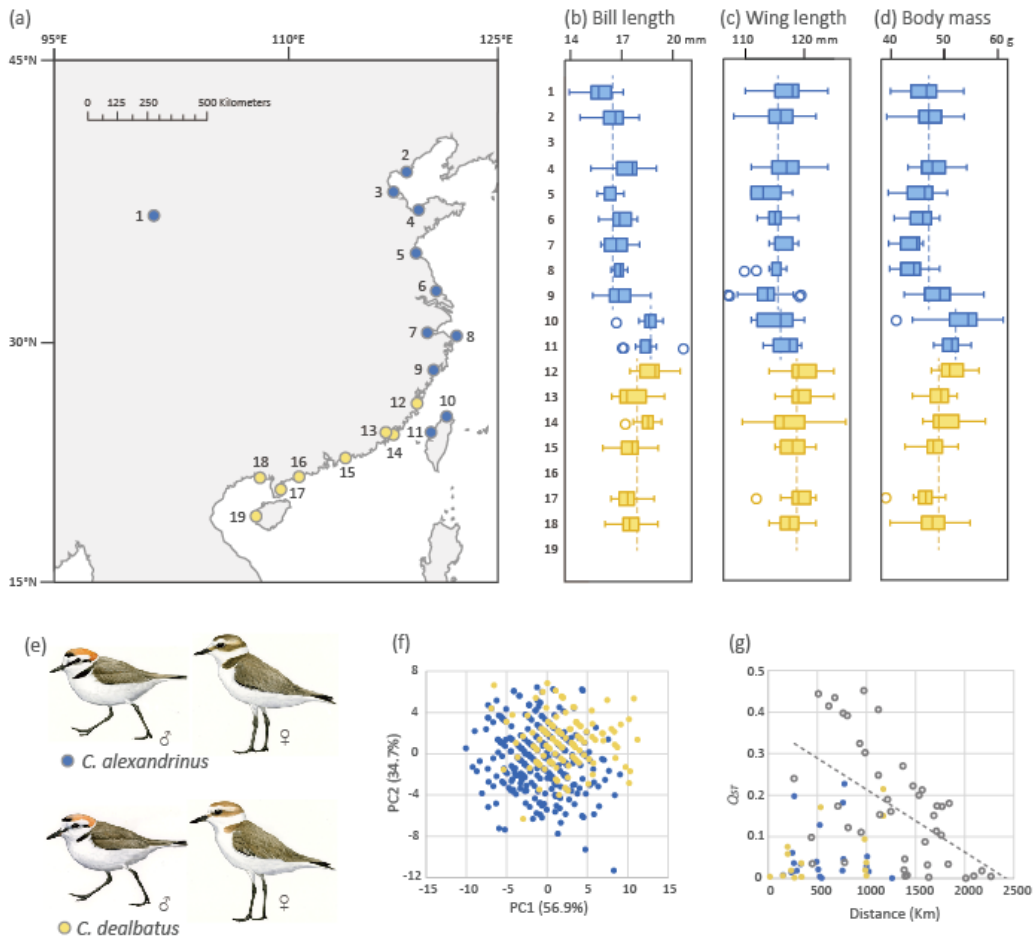
1060 that of *C. dealbatus* (yellow). (b) Distribution of the posterior probability that an
individual from one species is found within the niche region of the other species.

1062 Vertical lines for mean and 95% credible intervals are included in the histogram of
each overlap metric.

1064

FIGURE 1

1066



1068

FIGURE 2

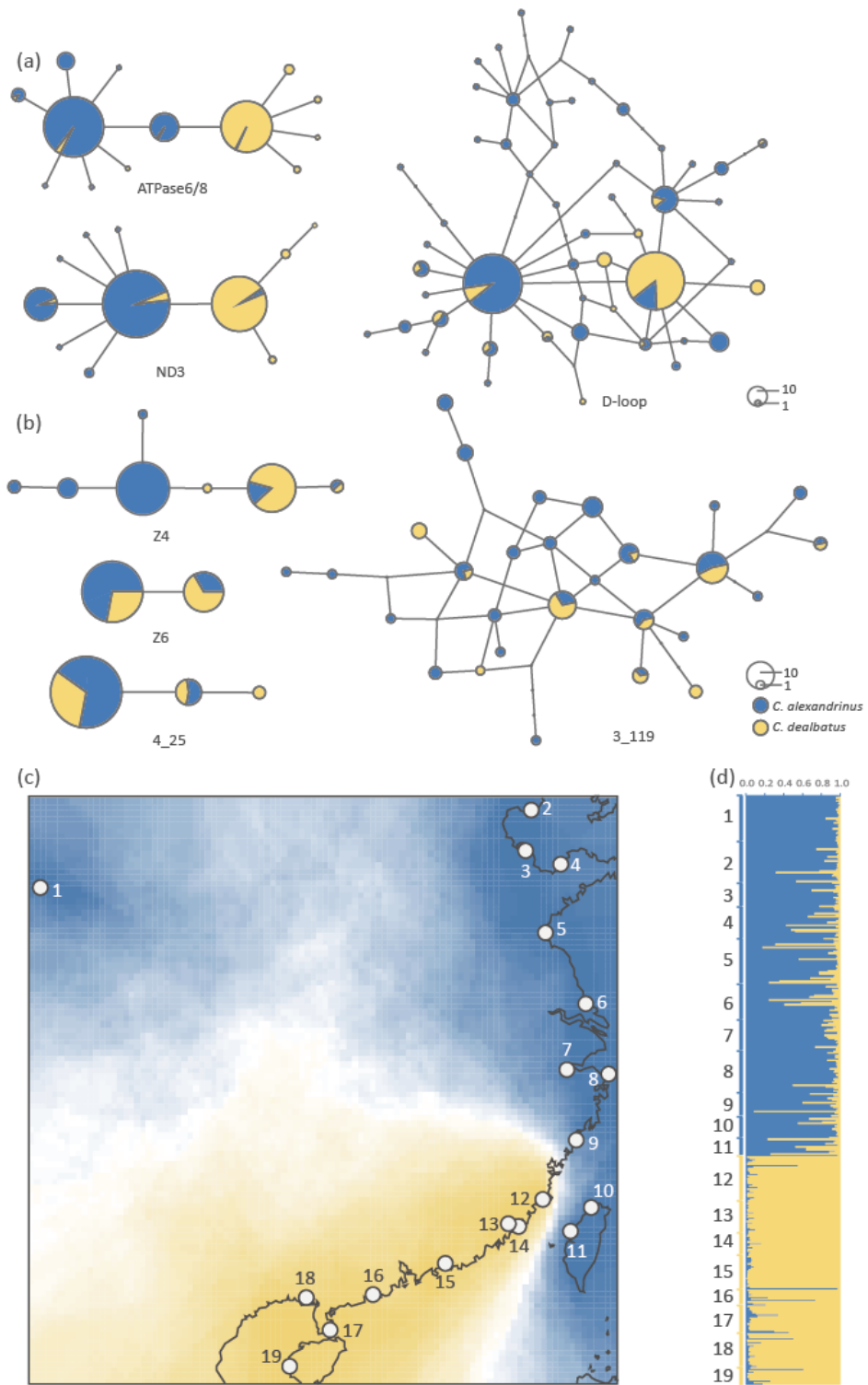
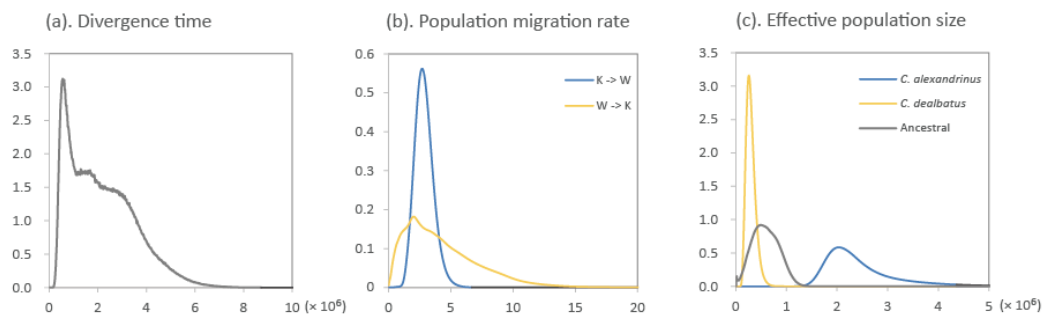


FIGURE 3

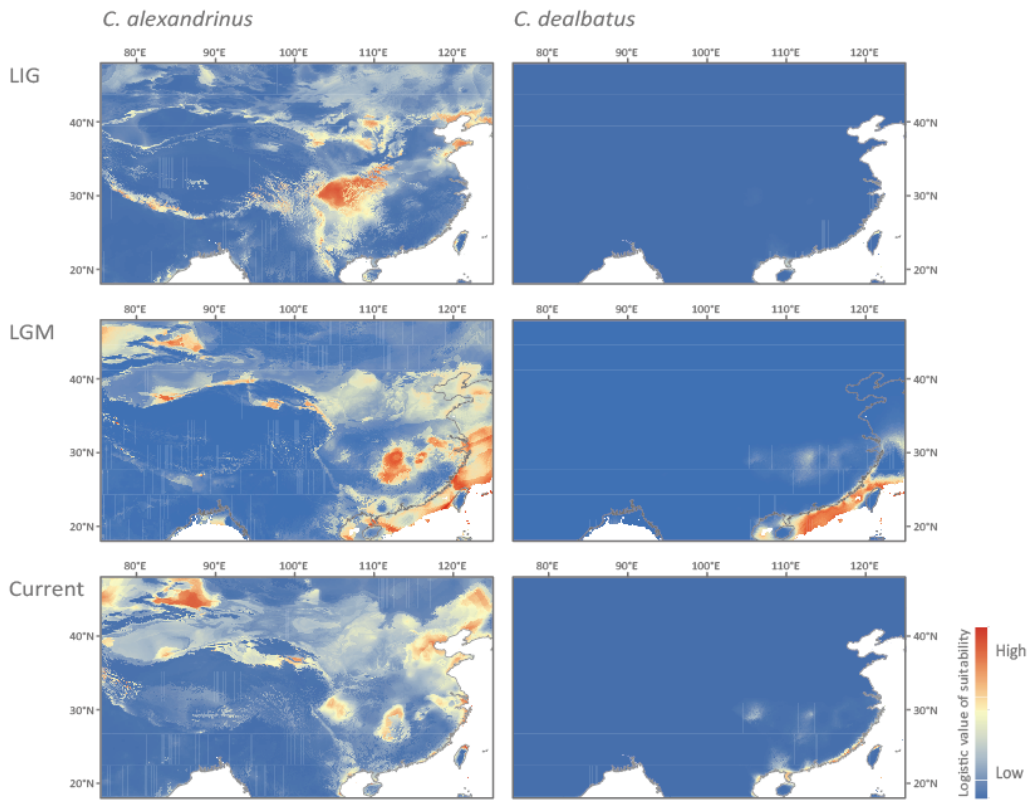
1072



1074

FIGURE 4

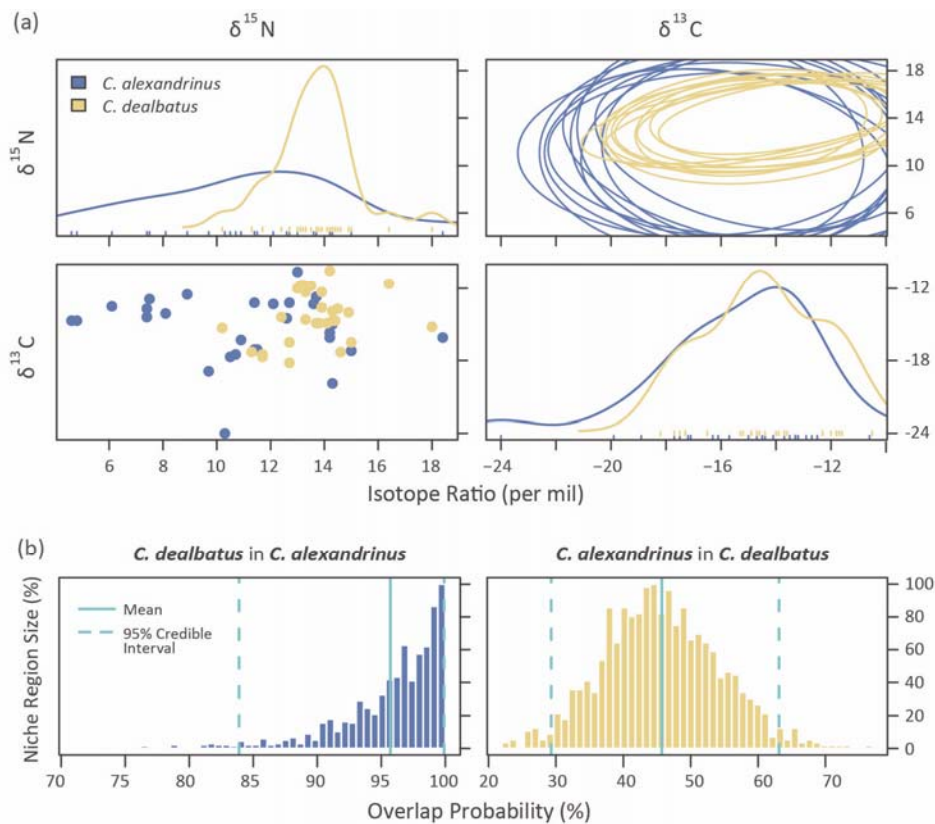
1076



1078

FIGURE 5

1080



1082

TABLE 1 Sampling localities and genetic polymorphism of *C. alexandrinus* and *C.*

1084 *dealbatus*. The number of individuals (*n*) analyzed for mtDNA, autosomal
 1086 microsatellites and nuclear exonic loci (nuDNA) are given. Site number corresponds to
 1088 the numbers in Figure 1. Estimates of *h*, number of haplotypes; *Hd*, haplotype diversity;
 1088 *π*, nucleotide diversity; *Tajima's D* value, *Ho*, observed heterozygosity; *He*, expected
 1088 heterozygosity were calculated for each locality and species.

Site	Latitude	Longitude	mtDNA					Microsatellites			nuDNA	
			<i>n</i>	<i>h</i>	<i>Hd</i>	<i>π</i>	<i>Tajima's D</i>	<i>n</i>	<i>Ho</i>	<i>He</i>	<i>n</i>	<i>Tajima's D</i>
<i>C. alexandrinus</i>			224	86	0.929	0.00181	-1.863*	219	0.723	0.802	30-40	0.216
1	Qinghai Lake	36.693	100.758	30	13	0.846	0.00119	-1.785	30	0.703	0.756	13-22
2	Tangshan	39.169	118.772	23	16	0.945	0.00171	-1.434	30	0.797	0.800	12-20
3	Cangzhou	38.471	117.682	14	8	0.868	0.00097	-0.871	16	0.774	0.791	
4	Weifang	37.131	119.484	21	14	0.895	0.00158	-1.687	22	0.671	0.787	
5	Lianyungang	34.742	119.243	28	20	0.963	0.00189	-1.166	30	0.697	0.777	
6	Nantong	32.575	121.043	25	12	0.913	0.00185	-0.016	26	0.731	0.796	
7	Zhoushan	29.991	122.151	19	11	0.924	0.00111	-0.141	20	0.746	0.779	
8	Ningbo	30.205	120.918	25	18	0.963	0.00179	-0.958	29	0.751	0.793	
9	Wenzhou	27.937	120.919	14	13	0.989	0.00161	-1.048	16	0.740	0.768	
10	Xinbei	25.862	119.614	14	6	0.736	0.00108	-0.971	30	0.672	0.700	2-8
11	Zhanghua	24.559	118.297	11	5	0.709	0.00076	-0.893	22	0.692	0.669	4-8
<i>C. dealbatus</i>			133	29	0.667	0.00086	-1.989*	131	0.714	0.758	23-28	0.326
12	Jinmen	24.448	118.600	13	7	0.731	0.00110	-1.362	15	0.733	0.703	5-8
13	Fuzhou	25.190	121.392	29	12	0.874	0.00108	-1.445	15	0.718	0.761	
14	Xiamen	24.162	120.402	18	6	0.699	0.00075	-1.532	12	0.755	0.748	
15	Shanwei	22.798	115.418	15	3	0.590	0.00039	0.221	23	0.669	0.696	
16	Yangjiang	21.589	111.758	10	5	0.822	0.00158	-0.144	11	0.713	0.718	
17	Zhanjiang	20.238	109.921	18	7	0.569	0.00099	-1.696	20	0.719	0.721	
18	Beihai	21.426	109.196	18	4	0.314	0.00044	-1.849*	23	0.692	0.695	18-12
19	Dongfang	19.234	109.804	12	2	0.167	0.00019	-1.141	12	0.763	0.679	
All			357	109	0.922	0.00216	-1.741	402	0.719	0.780	55-80	0.271

1090

TABLE 2 Hierarchical analyses of molecular variance (AMOVA) based on

concatenated mtDNA data and 13 microsatellite loci for *C. alexandrinus* and *C. dealbatus*. Samples were partitioned in three groupings: 2 groups (*C. alexandrinus* and *C. dealbatus*); 3 groups (*C. alexandrinus* continental populations and Taiwan island populations, *C. dealbatus*); 4 groups (*C. alexandrinus* inland (Qinghai Lake), *C. alexandrinus* coastal, *C. alexandrinus* Taiwan island, and *C. dealbatus*). *V_a*, genetic variation among groups; *V_b*, variation among populations within groups; *V_c*, variation within populations. Between-group genetic differentiation was highest when populations were partitioned into two groups (*C. alexandrinus* and *C. dealbatus*).

1100

	Grouping	<i>V_a/%</i>	<i>V_b/%</i>	<i>V_c/%</i>
mtDNA	2	49.712	8.491	41.797
	3	45.695	9.269	45.036
	4	41.782	10.296	47.922
microsatellites	2	2.416	1.798	95.786
	3	2.192	1.749	96.059
	4	1.917	1.776	96.307

1102 All *p* < 0.001

1104 **TABLE 3** Posterior mode, mean and range of 95% highest probability distribution
(HPD) of six demographic parameters inferred with IMa2p between *C. alexandrinus*
1106 and *C. dealbatus*. Divergence times (T) are given in million years ago (Ma). The
effective population size (N_e) of *C. alexandrinus* was about eight times that of *C.*
1108 *dealbatus*. Migration rate ($2NM$) into each species was about the same. K represents
Kentish Plover *C. alexandrinus*; W represents White-faced Plover *C. dealbatus*; A is
1110 the most recent common ancestor of two species.

Parameter	T/Ma	$N_e_w/10^6$	$N_e_k/10^6$	$N_e_A/10^6$	$2NM_{K \rightarrow W}$	$2NM_{W \rightarrow K}$
Mode	0.557	0.259	2.036	0.495	2.696*	2.005*
Mean	2.160	0.297	2.450	0.589	2.859	4.306
2.5% HPD	0.413	0.154	1.590	0.134	1.581	0.528
97.5% HPD	5.187	0.515	4.442	1.098	4.503	11.500

* $p < 0.001$

1112

1114